Portnov, A., Cook, A.E., and Vadakkepuliyambatta, S., 2021, Diverse gas composition controls the Moby-Dick gas hydrate system in the Gulf of Mexico: Geology, v. 49, https://doi.org/10.1130/G49310.1

SUPPLEMENTARY INFORMATION

1. Seismic and well log data

We used a time-migrated 3D seismic survey, B-20-92-LA, acquired in 1992 and 2D line W-LS-389A_E publicly available at the National Archive of Marine Seismic Surveys, https://walrus.wr.usgs.gov/NAMSS/. The seismic data has American zero-phase polarity where an increase in acoustic impedance corresponds to peak-leading reflections. Signal frequency spectra of the 3D data is 7 - 65 Hz, resulting in an average vertical resolution of ~7 m at the depth of the gas hydrate system. The depositional system, BSR, and gas hydrate accumulations were characterized using a suite of seismic attributes (root-mean-square amplitudes, average positive and negative amplitudes, frequency spectral decomposition). Resistivity, gamma ray, gas chromatographic logs, permit documents, and drilling operations reports from the DGE well (API 608114053100) were acquired from the US BSEE (https://www.data.bsee.gov/). The velocity model for the seismic-well tie and all time-depth conversions was based on the density and velocity functions derived for marine mud sediments in Cook and Sawyer (2015).

2. Geothermal gradient

Geothermal gradients over the mapped BSR surface are calculated based on the depth of the BSR below the seafloor. Thermal conductivity of the sediments above the BSR is assumed laterally uniform based on the uniform stratigraphy across the study area. A water column velocity of 1500 m/s and an average sediment velocity of 1860 m/s were used to convert between TWT and depth. Assuming the BSR represents the theoretical base of GHSZ, temperature at the mapped BSR is calculated using the phase-boundary for 100% C_1 gas mix and 35 g L^{-1} pore-water salinity (Sloan and Koh, 2008). The thermal gradient (dT/dz) at each location was estimated using the following equation:

$$\frac{dT}{dz} = \frac{T_{BSR} - T_{water}}{\Delta z}$$

where T_{BSR} is the temperature at the BSR, T_{water} is the bottom-water temperature (assumed to be 4.2 °C), and Δz is the depth of mapped BSR below the seafloor.

3. Gamma ray, resistivity and density log data from the Deep Gulf Energy well (API 608114053100).

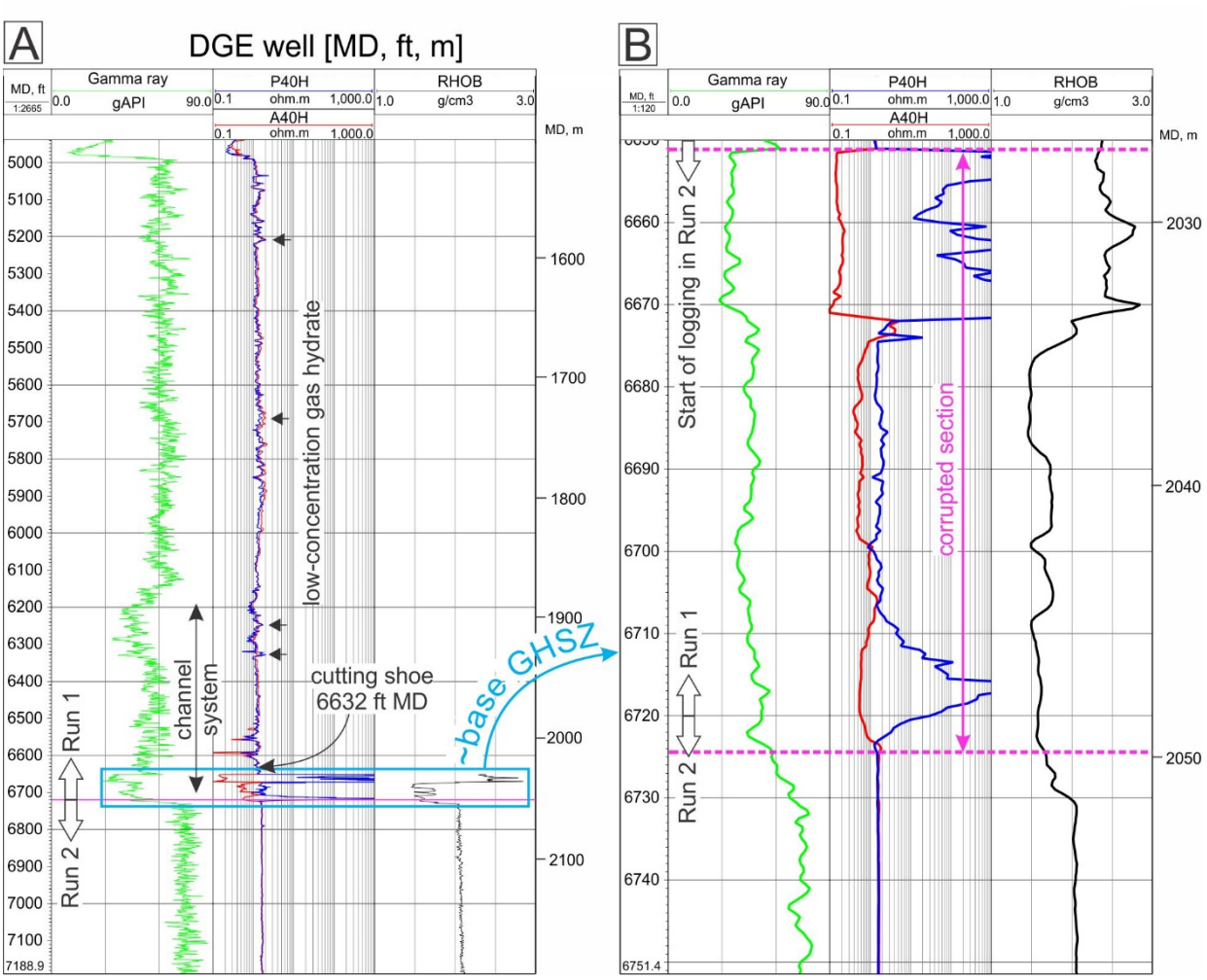

Supplementary Figure 1. A) Gamma ray, resistivity (P40H and A40H) and density logs in DGE well. Gamma ray shows the channel system. Resistivity spikes above the base of GHSZ indicate low-concentration gas hydrate. B) Zoom of the corrupted section at the approximate base of GHSZ where casing between Run 1 and Run 2 was installed. Note, MD is measured depth from the rig floor in ft (left) and m (right), kelly bushing is 79 ft (24 m).

4. Potential effects of sedimentation and seismic velocity on the BSR depth.

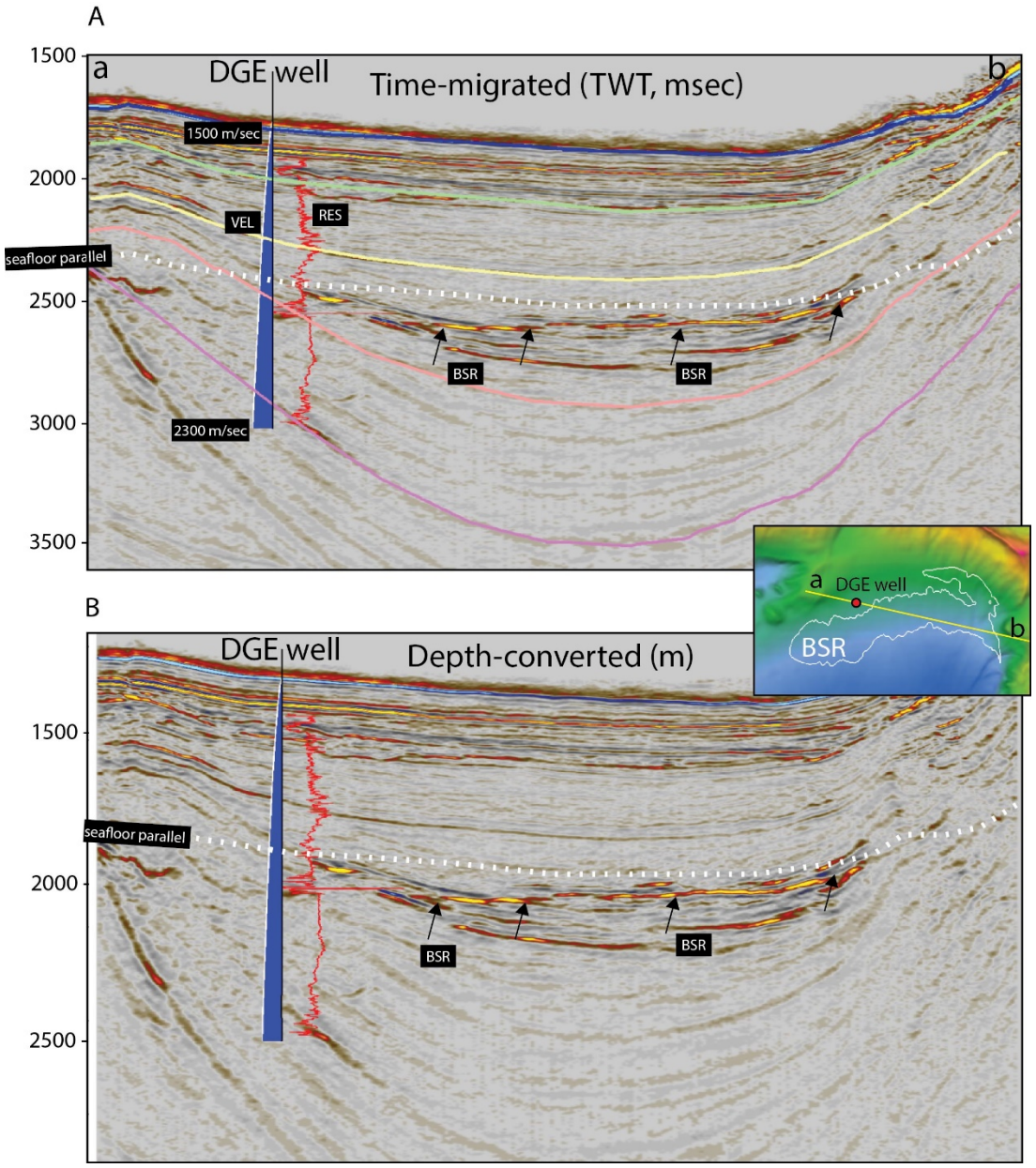

Supplementary Figure 2. (A) Time-migrated seismic section a-b (location is shown in the inset) shows uniform stratigraphic bedding above the BSR, indicating no sedimentation-driven cooling effects potentially causing the deeper BSR in the west. Seismic velocity profile adapted for the DGE well tie was applied to depth-convert the seismic section using 5 major horizons (color lines). (B) Depth-converted seismic section a-b showing BSR configuration consistent with the time-migrated section indicating that velocity effects are not responsible for the varying BSR depth.

5. Gas composition data from the Deep Gulf Energy well (API 608114053100).

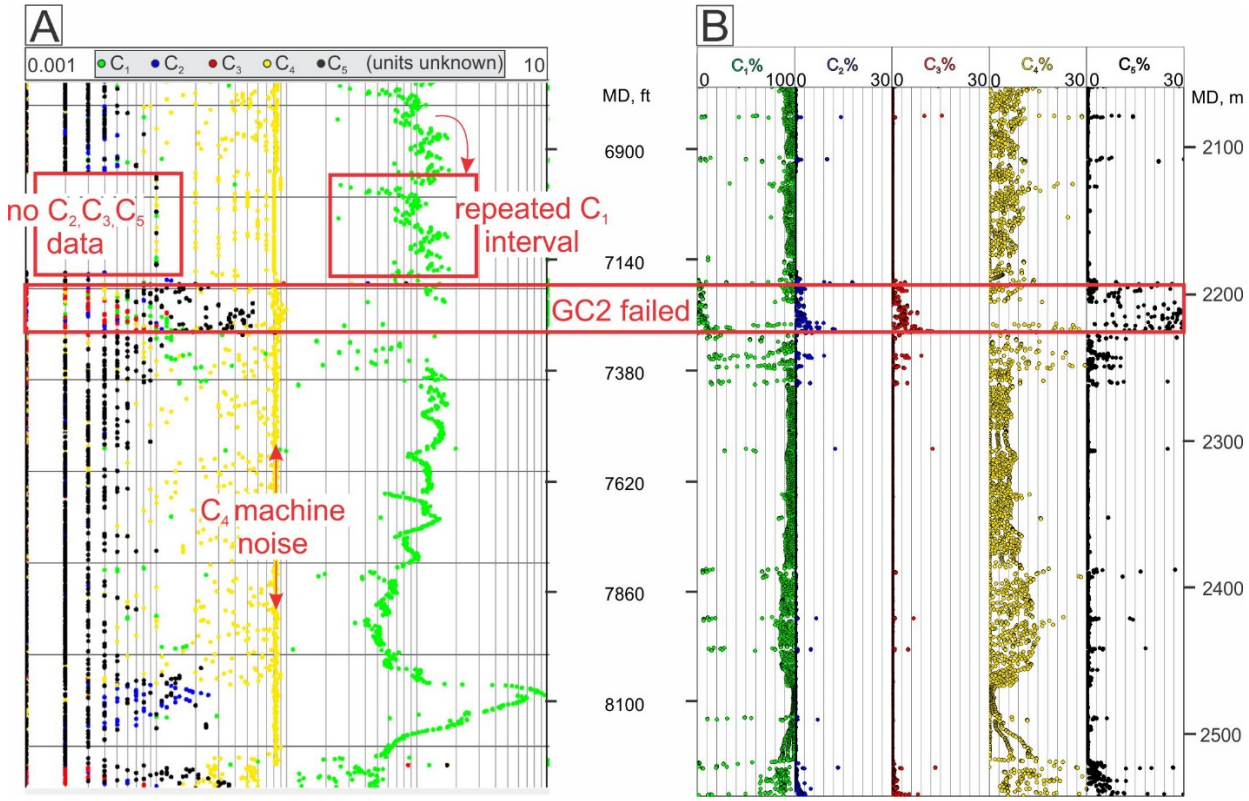

Supplementary Figure 3. Gas composition in absolute values (A) (units on the log scale are unknown) and in % from the total gas composition (B) in DGE well. Gas composition data are not reliable and cannot be used due to compromised and/or absent gas chromatographic measurements and machine failures in various intervals below the GHSZ.

References cited

Cook, A., and Sawyer, D., 2015, The mud-sand crossover on marine seismic data: Geophysics, v. 80, p. A109–A114, doi:10.1190/GEO2015-0291.1.

Kominz, M.A., Patterson, K., and Odette, D., 2011, Lithology dependence of porosity in slope and deep marine sediments: Journal of Sedimentary Research, v. 81, p. 730–742, doi:10.2110/jsr.2011.60.

Phillips, S.C., Flemings, P.B., Holland, M.E., Schultheiss, P.J., Waite, W.F., Jang, J., Petrou, E.G., and Hammon, H., 2020, High concentration methane hydrate in a silt reservoir from the deep-water Gulf of Mexico: AAPG Bulletin, v. 104, p. 1971–1995, doi:10.1306/01062018280.

Ruppel, C.D., 2011, Methane Hydrates and Contemporary Climate Change: Nature Education Knowledge, v. 3 (10), 29, http://www.nature.com/scitable/knowledge/library/methane-hydrates-and-contemporary-climatechange-24314790, Online only.